

ADVANCED FUNCTIONAL MATERIALS

Supporting Information

for *Adv. Funct. Mater.*, DOI: 10.1002/adfm.201909983

Electronic Structure and Optoelectronic Properties of Bismuth
Oxyiodide Robust against Percent-Level Iodine-, Oxygen-,
and Bismuth-Related Surface Defects

*Tahmida N. Huq, Lana C. Lee, Lissa Eyre, Weiwei Li, Robert
A. Jagt, Chaewon Kim, Sarah Fearn, Vincenzo Pecunia, Felix
Deschler, Judith L. MacManus-Driscoll, and Robert L. Z.
Hoye**

Supporting Information

Electronic Structure and Optoelectronic Properties of Bismuth Oxyiodide Robust Against Percent-Level Iodine-, Oxygen- and Bismuth-Related Surface Defects

*Tahmida N. Huq,[†] Lana C. Lee,[†] Lissa Eyre, Weiwei Li, Robert A. Jagt, Chaewon Kim, Sarah Fearn, Vincenzo Pecunia, Judith L. MacManus-Driscoll, and Robert L. Z. Hoye**

T. N. Huq, Dr. L. C. Lee, Dr. W. Li, R. A. Jagt, Prof. J. L. MacManus-Driscoll, Dr. R. L. Z. Hoye
Department of Materials Science and Metallurgy, University of Cambridge, 27 Charles Babbage Road, Cambridge CB3 0FS, UK

L. Eyre
Department of Physics, University of Cambridge, JJ Thomson Ave, Cambridge CB3 0HE, UK

L. Eyre, Dr. F. Deschler
Walter Schottky Institute, Department of Physics, Technical University of Munich
Am Coulombwall 4, 85748 Garching, Germany

Dr. C. Kim, Dr. V. Pecunia
Institute of Functional Nano & Soft Materials (FUNSOM), Jiangsu Key Laboratory for Carbon-Based Functional Materials & Devices, Soochow University, 199 Ren'ai Road, Suzhou, 215123, Jiangsu, P. R. China

Dr. S. Fearn, Dr. R. L. Z. Hoye
Department of Materials, Imperial College London, Exhibition Road, London SW7 2AZ, UK
Email: r.hoye@imperial.ac.uk

[†] These authors contributed equally

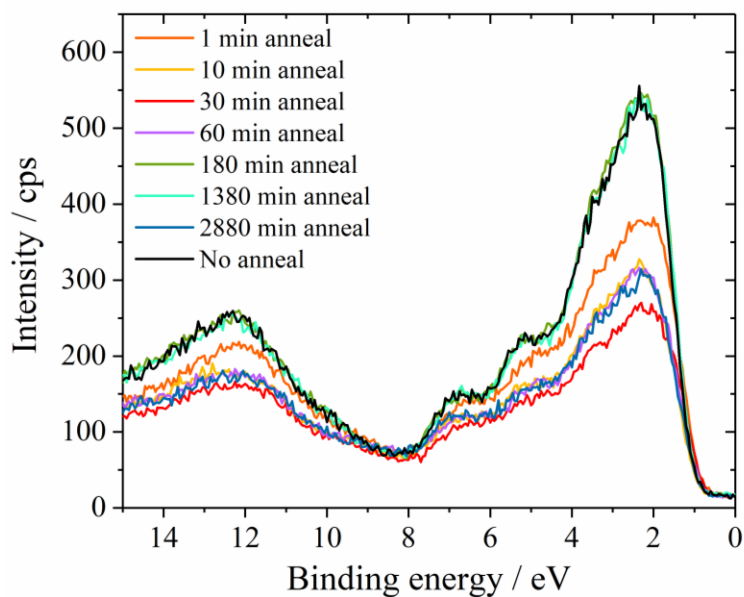


Figure S1. Valence band spectra of BiOI without annealing and with vacuum annealing for different periods of time

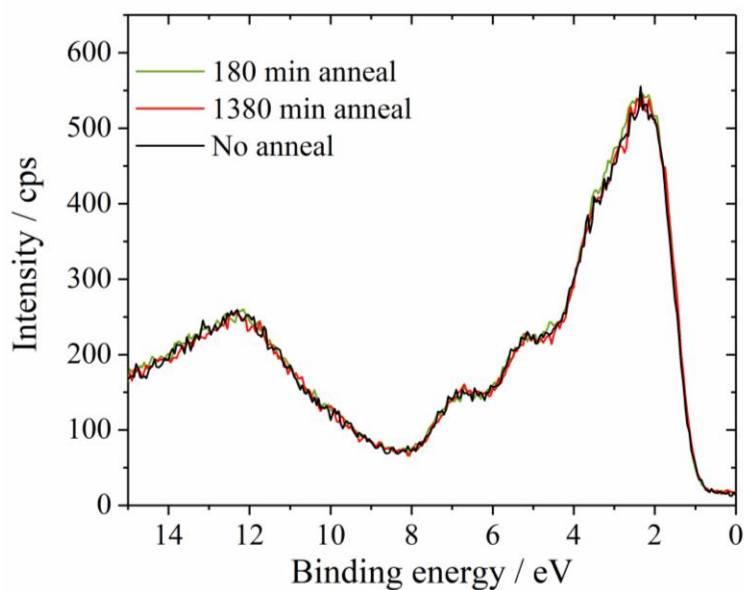


Figure S2. Comparison of the normalized valence band spectra of BiOI without annealing and after 3 h (180 min) and 23 h (1380 min) vacuum annealing.

Table S1. Composition of BiOI thin films without vacuum and annealing vs. with 10 min vacuum annealing measured by energy dispersive X-ray spectrophotometry (EDX). Note that only the Bi and I content are shown due to the difficulty in accurately measuring the O content by EDX.

Non-annealed BiOI							
	Region 1 (at%)	Region 2 (at%)	Region 3 (at%)	Region 4 (at%)	Region 5 (at%)	Average (at%)	Uncertainty
Bi (M-series)	43.590	43.790	43.890	43.050	43.400	43.544	0.299
I (L-series)	42.740	42.400	42.030	41.840	42.890	42.38	0.401
Ratio (I:Bi): 0.973						Uncertainty in ratio: 0.011	
10 min annealed BiOI							
	Region 1 (at%)	Region 2 (at%)	Region 3 (at%)	Region 4 (at%)	Region 5 (at%)	Average (at%)	Uncertainty
Bi (M-series)	43.370	41.970	43.640	44.590	43.280	43.370	0.840
I (L-series)	41.940	43.550	41.530	40.820	42.750	42.118	0.950
Ratio (I:Bi) : 0.971						Uncertainty in ratio: 0.029	

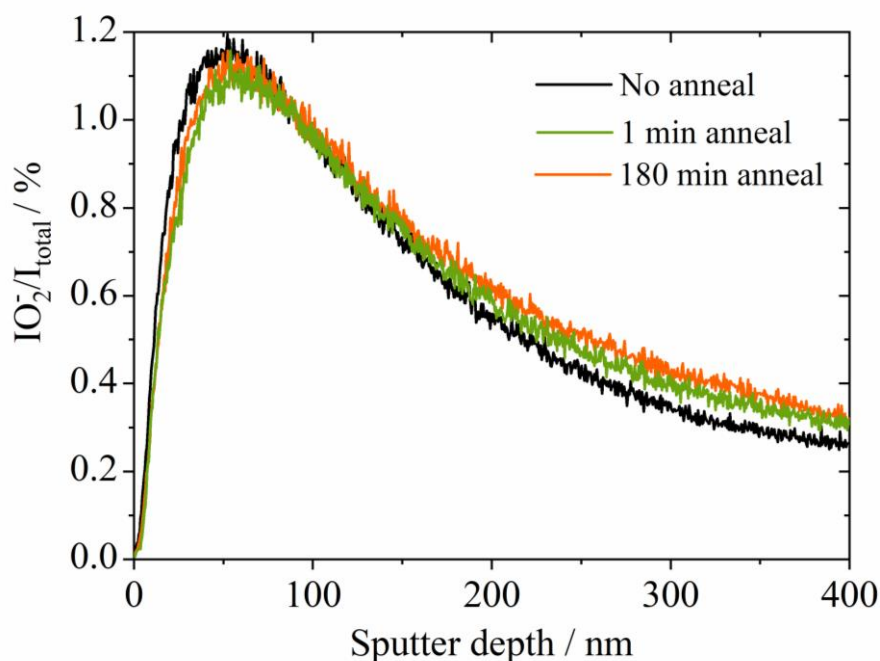


Figure S3. Normalised IO_2^- profiles measured with ToF-SIMS of the unannealed, 1 min annealed and 180 min annealed samples.

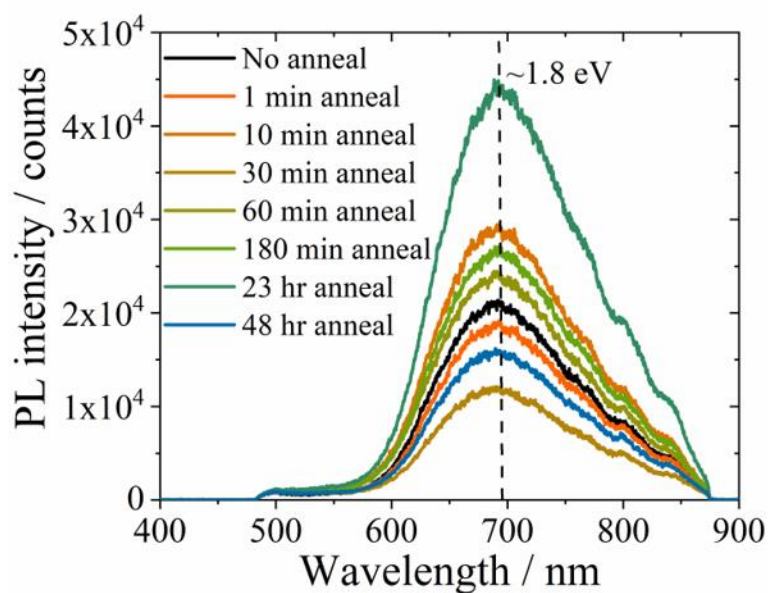


Figure S4. Photoluminescence spectra of unannealed and vacuum-annealed BiOI films

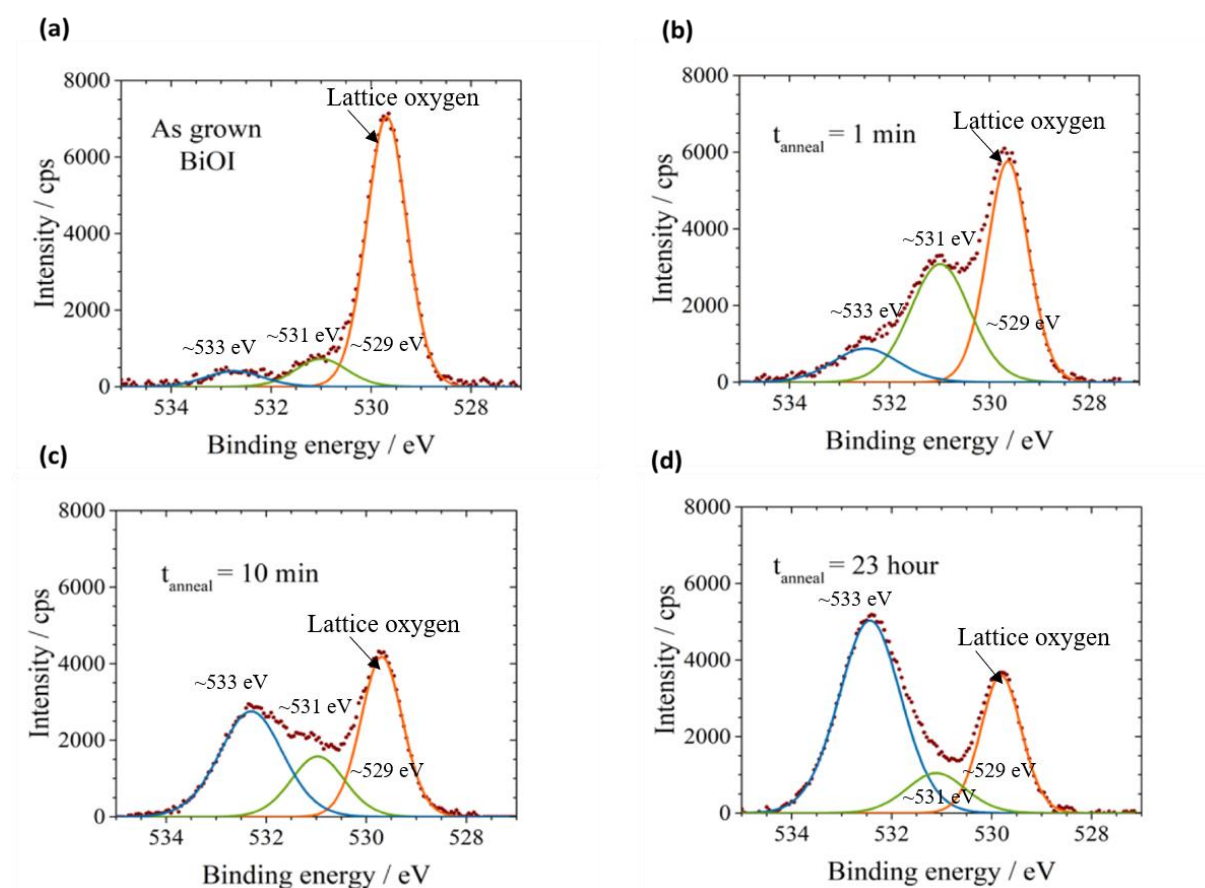


Figure S5. O1s core spectra of (a) as grown BiOI, (b) BiOI vacuum annealed for 1 minute, (c) BiOI vacuum annealed for 10 min and (d) BiOI vacuum annealed for 23 h at 100 °C, 25 Pa.

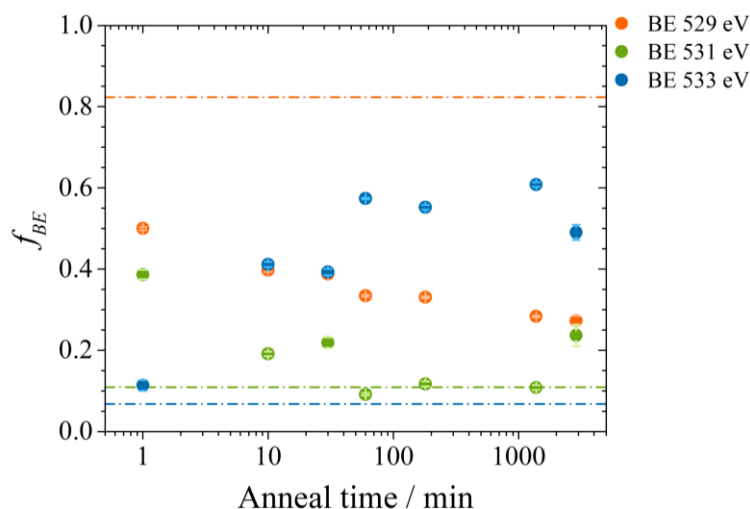


Figure S6. Plot shows the change in fractional contribution (f_{BE}) of the peaks at binding energies 529 eV, 531 eV and 533 eV to the O 1s spectra as vacuum annealing time increased. The dashed lines show the fractional contribution of the peaks at binding energy 529 eV (orange), 531 eV (green) and 533 eV (blue) to the O 1s spectrum for an as grown BiOI sample.

Table S2. The conditions used to grow mixed phase samples **A**, **B** and **C**, the color of the film and the phases present as determined by XRD. Powder Diffraction Files (PDF) were used to identify BiOI (00-010-0445), Bi₅O₇I (00-038-0669), BiO₉I₃ (00-058-0583) and Bi₂O_{2.33} (00-027-0051) and β -Bi₂O₃ (00-001-0709).

Sample ID	Conditions		Film color	Phases present
	Temperature / °C	O ₂ flow / %		
A	450	5	Red	BiOI, Bi ₅ O ₇ I
B	450	50	Red	BiOI, Bi ₅ O ₇ I, Bi ₂ O _{2.33}
C	400	50	Yellow	BiOI, BiO ₉ I ₃ , Bi ₅ O ₇ I, β -Bi ₂ O ₃

Table S3. The estimated Fermi level (E_F) to valence band (VB) offset of mixed phase samples A, B, and C, as predicted from the XPS valence band spectra.

Sample	$E_F - VB / eV$
A	0.55
B	0.87
C	1.24

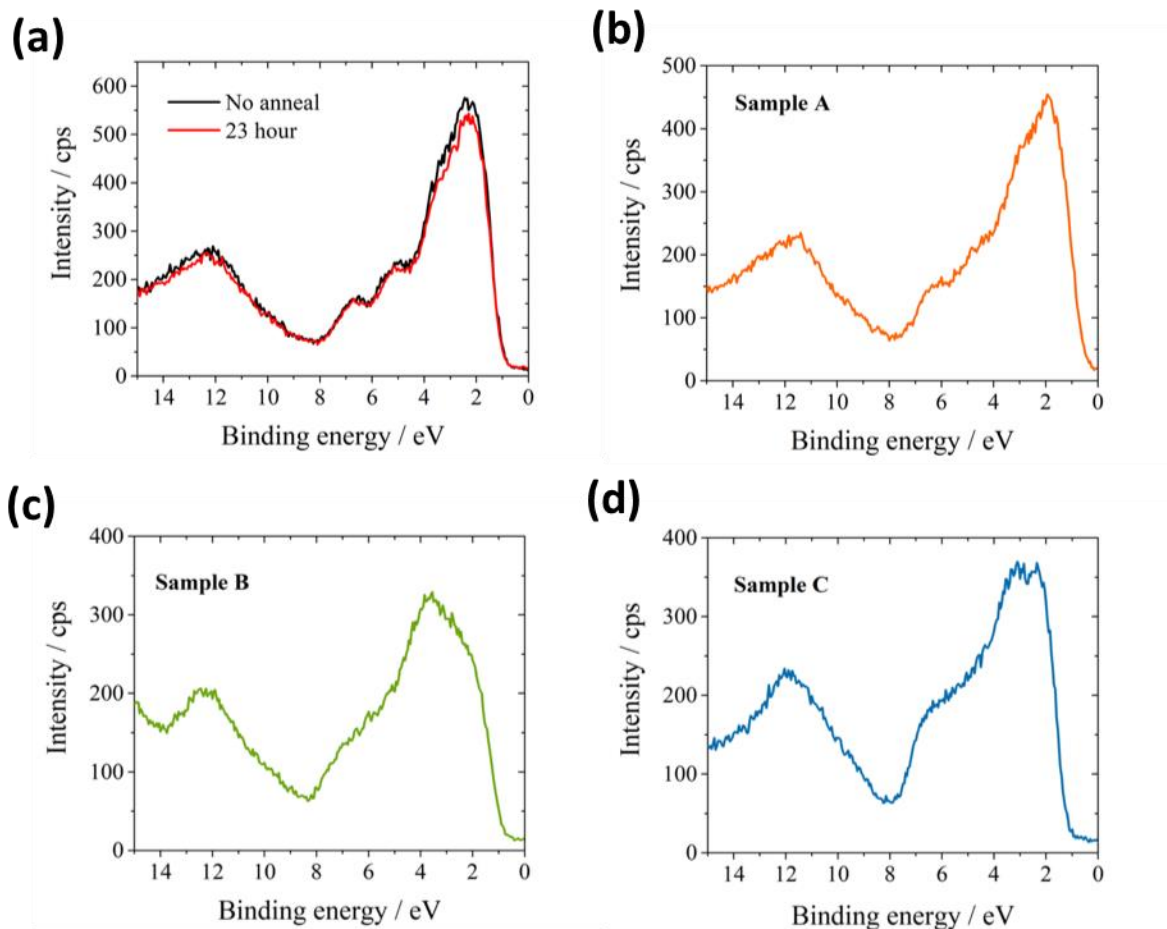


Figure S7. The valence band spectra for a) as-deposited BiOI (black line) and BiOI vacuum annealed for 23 hours at 100 °C, 25 Pa (red line), b) sample A, a mixed phase sample containing BiOI and Bi₅O₇I, c) sample B, a mixed phase sample containing BiOI, Bi₅O₇I and Bi₂O_{2.33}, and d) sample C, a mixed phase sample containing BiOI, BiO₉I₃, Bi₅O₇I and β -Bi₂O₃.

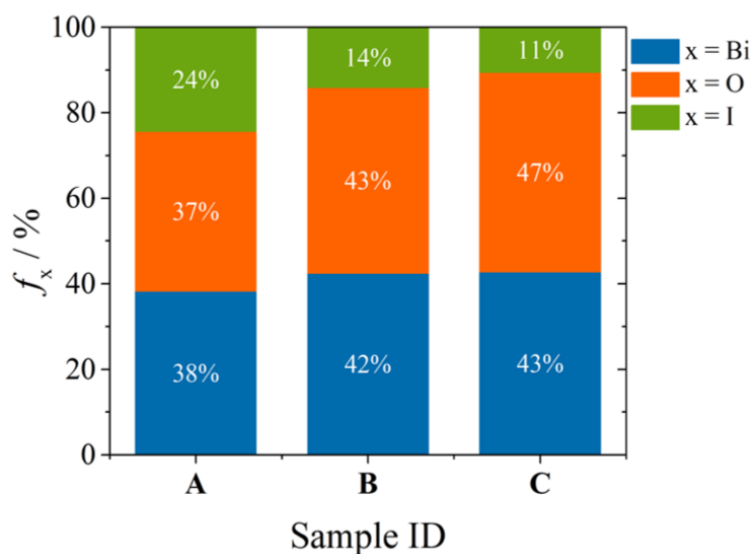


Figure S8. The composition of samples A, B and C determined using the areas of the XPS core level spectra, accounting for the relative sensitivity factor for each orbital.

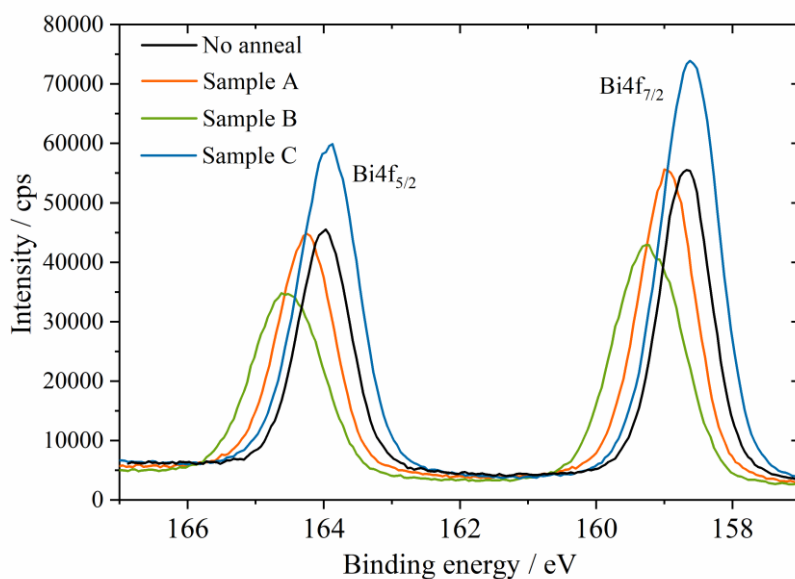


Figure S9. Bi 4*f* core level spectra of non-annealed and mixed phase samples

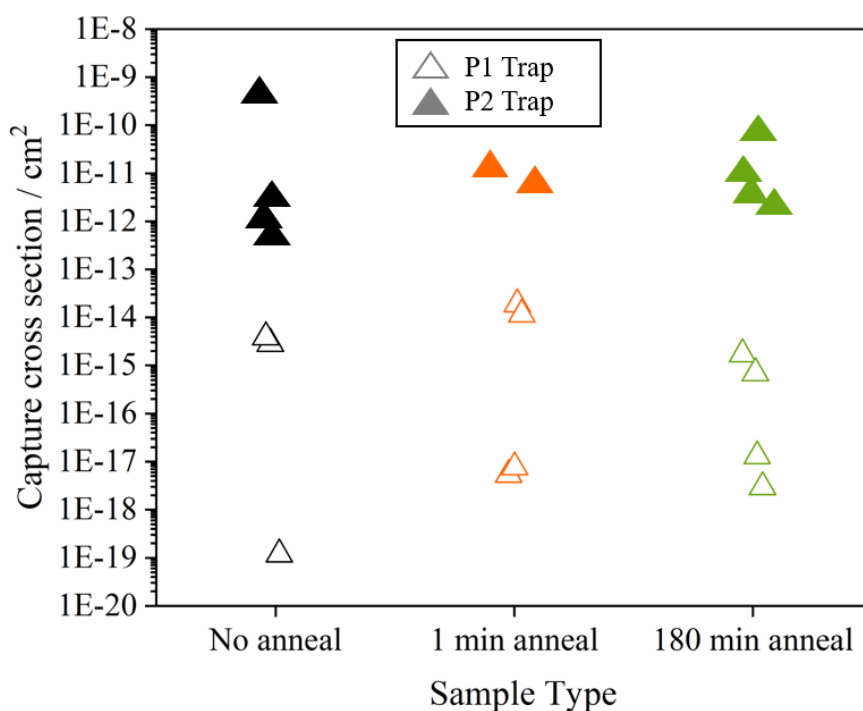


Figure S10. PICTS data of the capture cross-section for vacuum annealed samples. Two deep levels were found in the PICTS spectra (see Figure S11) and these are labelled P1 and P2. The open points are for the P1 trap found in each sample, while the closed points are for the P2 trap in each sample

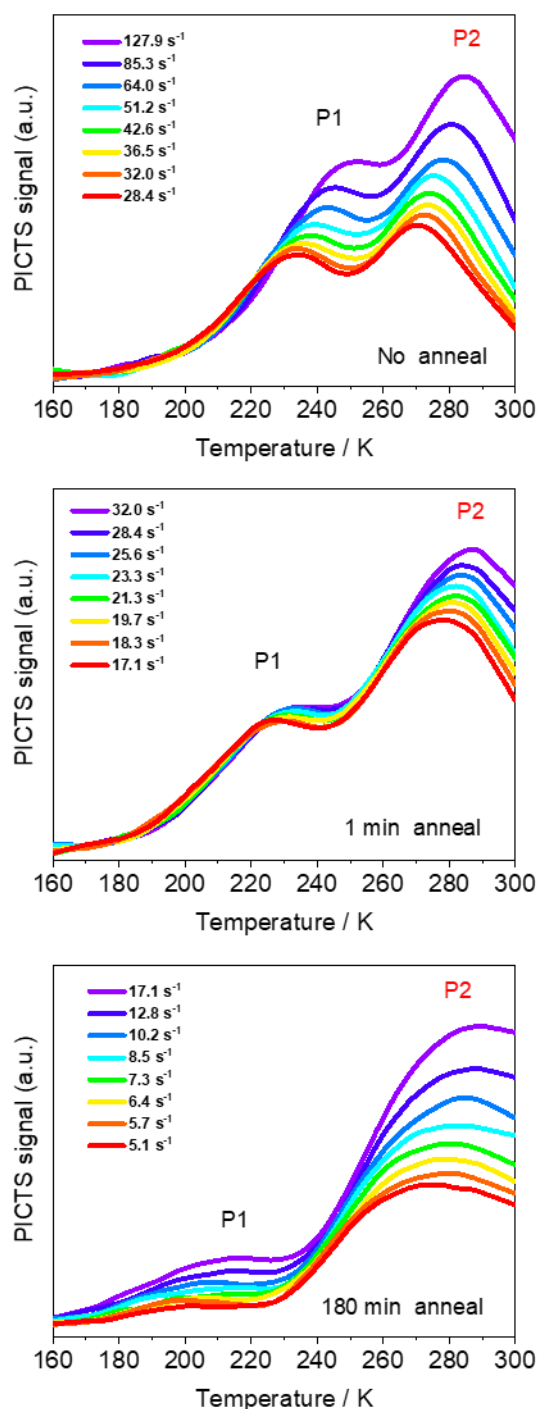


Figure S11. PICTS spectra at various rate window values for unannealed, 1 min annealed, and 180 min annealed BiOI samples. Two thermally-activated peaks, labelled as P1 and P2, are apparent, which can be assigned to two deep levels. These spectra were determined through a boxcar-type scheme from the measured current transients ensuing trap-filling pulses.^[1] In brief, the difference between the device current at selected times t_1 and t_2 gives the PICTS signal $\Delta i = i(t_1) - i(t_2)$. The rate window is defined as $e_n = \ln(t_2/t_1)/(t_2 - t_1)$. By plotting the PICTS signal for various rate window values, the PICTS spectra shown here are obtained

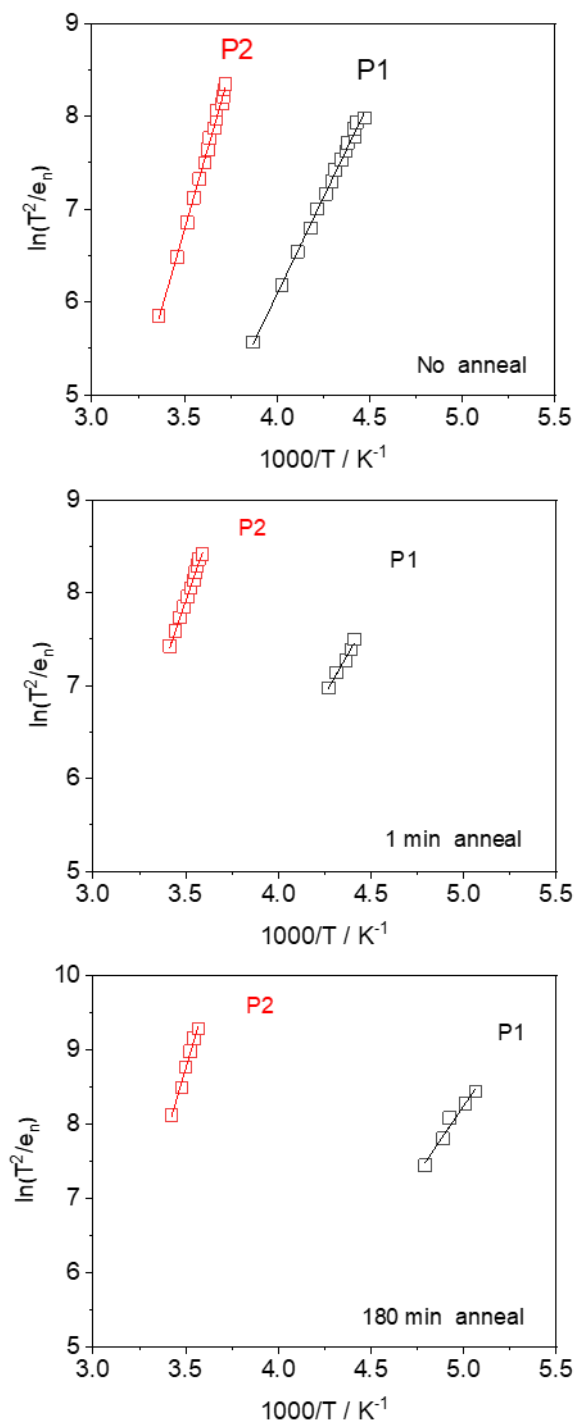


Figure S12. Arrhenius plots extracted from the PICTS spectra shown in Figure S11. In brief, these were derived from the temperature and rate window values of the PICTS spectra peaks in Figure S11, consistently with standard PICTS methodology.^[1] The deep level energies for P1 and P2 were determined from the slopes of the traces shown here, while cross-sections were extracted from their intercepts

References

[1] A. Erol, M. Ç. Arıkan, in *Semiconductor Research* (Eds.: A. Patane, N. Balkan), Springer, Berlin, Heidelberg, Germany **2012**, pp. 333–365.